

1-1-2009

Measurement of Direct $f_0(980)$ Photoproduction on the Proton

M. Battaglieri

Angela Biselli

Fairfield University, abiselli@fairfield.edu

CLAS Collaboration

Copyright American Physical Society Publisher final version available at <http://prl.aps.org/pdf/PRL/v102/i10/e102001>

Peer Reviewed

Repository Citation

Battaglieri, M.; Biselli, Angela; and CLAS Collaboration, "Measurement of Direct $f_0(980)$ Photoproduction on the Proton" (2009). *Physics Faculty Publications*. 54.
<http://digitalcommons.fairfield.edu/physics-facultypubs/54>

Published Citation

M. Battaglieri et al. [CLAS Collaboration], "Measurement of Direct $f_0(980)$ Photoproduction on the Proton," *Physical Review Letters* 102.10 (2009) DOI: 10.1103/PhysRevLett.102.102001

This Article is brought to you for free and open access by the Physics Department at DigitalCommons@Fairfield. It has been accepted for inclusion in Physics Faculty Publications by an authorized administrator of DigitalCommons@Fairfield. For more information, please contact digitalcommons@fairfield.edu.

Measurement of Direct $f_0(980)$ Photoproduction on the Proton

M. Battaglieri,¹ R. De Vita,¹ A. P. Szczepaniak,² K. P. Adhikari,³⁴ M. Aghasyan,¹⁹ M. J. Amarian,³⁴ P. Ambrozewicz,¹⁴ M. Anghinolfi,¹ G. Asryan,⁴⁷ H. Avakian,⁴¹ H. Bagdasaryan,³⁴ N. Baillie,⁴⁶ J. P. Ball,⁴ N. A. Baltzell,⁴⁰ V. Batourine,^{26,41} I. Bedlinskiy,²¹ M. Bellis,⁷ N. Benmouna,¹⁶ B. L. Berman,¹⁶ L. Bibrzycki,²⁸ A. S. Biselli,¹³ C. Bookwalter,¹⁵ S. Bouchigny,²⁰ S. Boiarinov,⁴¹ R. Bradford,⁷ D. Branford,¹² W. J. Briscoe,¹⁶ W. K. Brooks,^{41,43} S. Bültmann,³⁴ V. D. Burkert,⁴¹ J. R. Calarco,²⁹ S. L. Careccia,³⁴ D. S. Carman,⁴¹ L. Casey,⁸ S. Chen,¹⁵ L. Cheng,⁸ E. Clinton,²⁷ P. L. Cole,¹⁸ P. Collins,⁴ D. Crabb,⁴⁵ H. Crannell,⁸ V. Crede,¹⁵ J. P. Cummings,³⁵ D. Dale,¹⁸ A. Daniel,³³ N. Dashyan,⁴⁷ R. De Masi,⁹ E. De Sanctis,¹⁹ P. V. Degtyarenko,⁴¹ A. Deur,⁴¹ S. Dhamija,¹⁴ K. V. Dharmawardane,³⁴ R. Dickson,⁷ C. Djalali,⁴⁰ G. E. Dodge,³⁴ J. Donnelly,¹⁷ D. Doughty,^{10,41} M. Dugger,⁴ O. P. Dzyubak,⁴⁰ H. Egiyan,^{41,29} K. S. Egiyan,⁴⁷ L. El Fassi,³ L. Elouadrhiri,⁴¹ P. Eugenio,¹⁵ G. Fedotov,³⁹ R. Fersch,⁴⁶ T. A. Forest,¹⁸ A. Fradi,²⁰ M. Y. Gabrielyan,¹⁴ L. Gan,³¹ M. Garçon,⁹ A. Gasparian,³² G. Gavalian,^{29,34} N. Gevorgyan,⁴⁷ G. P. Gilfoyle,³⁷ K. L. Giovanetti,²³ F. X. Girod,^{9,41} O. Glamazdin,²⁵ J. Goett,³⁵ J. T. Goetz,⁵ W. Gohn,¹¹ E. Golovatch,³⁹ C. I. O. Gordon,¹⁷ R. W. Gothe,⁴⁰ L. Graham,⁴⁰ K. A. Griffioen,⁴⁶ M. Guidal,²⁰ N. Guler,³⁴ L. Guo,⁴¹ V. Gyurjyan,⁴¹ C. Hadjidakis,²⁰ K. Hafidi,³ H. Hakobyan,^{47,41,43} R. S. Hakobyan,⁸ C. Hanretty,¹⁵ J. Hardie,^{10,41} N. Hassall,¹⁷ D. Heddle,^{10,41} F. W. Hersman,²⁹ K. Hicks,³³ I. Hleiqawi,³³ M. Holtrop,²⁹ C. E. Hyde,³⁴ Y. Ilieva,^{16,40} D. G. Ireland,¹⁷ B. S. Ishkhanov,³⁹ E. L. Isupov,³⁹ M. M. Ito,⁴¹ D. Jenkins,⁴⁴ H. S. Jo,²⁰ J. R. Johnstone,¹⁷ K. Joo,¹¹ H. G. Juengst,^{16,34,8} T. Kageya,⁴¹ N. Kalantarians,³⁴ D. Keller,³³ J. D. Kellie,¹⁷ M. Khandaker,³⁰ P. Khetarpal,³⁵ W. Kim,²⁶ A. Klein,³⁴ F. J. Klein,⁸ A. V. Klimenko,³⁴ P. Konczykowski,⁹ M. Kossov,²¹ Z. Krahn,⁷ L. H. Kramer,^{14,41} V. Kubarovsky,^{35,41} J. Kuhn,⁷ S. E. Kuhn,³⁴ S. V. Kuleshov,^{21,43} V. Kuznetsov,²⁶ J. Lachniet,^{7,34} J. M. Laget,^{9,41} J. Langheinrich,⁴⁰ D. Lawrence,²⁷ T. Lee,²⁹ L. Lesniak,²⁸ Ji Li,³⁵ K. Livingston,¹⁷ M. Lowry,⁴¹ H. Y. Lu,⁴⁰ M. MacCormick,²⁰ S. Malace,⁴⁰ N. Markov,¹¹ P. Mattione,³⁶ M. E. McCracken,⁷ B. McKinnon,¹⁷ B. A. Mecking,⁴¹ J. J. Melone,¹⁷ M. D. Mestayer,⁴¹ C. A. Meyer,⁷ T. Mibe,³³ K. Mikhailov,²¹ T. Mineeva,¹¹ R. Minehart,⁴⁵ M. Mirazita,¹⁹ R. Miskimen,²⁷ V. Mochalov,²² V. Mokeev,^{39,41} B. Moreno,²⁰ K. Moriya,⁷ S. A. Morrow,^{20,9} M. Moteabbed,¹⁴ E. Munevar,¹⁶ G. S. Mutchler,³⁶ P. Nadel-Turonski,⁸ I. Nakagawa,³⁸ R. Nasseripour,^{14,40,16} S. Niccolai,²⁰ G. Niculescu,²³ I. Niculescu,²³ B. B. Niczyporuk,⁴¹ M. R. Niroula,³⁴ R. A. Niyazov,^{41,35} M. Nozar,⁴¹ M. Osipenko,^{1,39} A. I. Ostrovidov,¹⁵ K. Park,^{26,40} S. Park,¹⁵ E. Pasyuk,⁴ M. Paris,^{16,41} C. Paterson,¹⁷ S. Anefalos Pereira,¹⁹ J. Pierce,⁴⁵ N. Pivnyuk,²¹ D. Pocanic,⁴⁵ O. Pogorelko,²¹ S. Pozdniakov,²¹ J. W. Price,⁶ Y. Prok,¹⁰ D. Protopopescu,¹⁷ B. A. Raue,^{14,41} G. Riccardi,¹⁵ G. Ricco,¹ M. Ripani,¹ B. G. Ritchie,⁴ G. Rosner,¹⁷ P. Rossi,¹⁹ F. Sabatié,⁹ M. S. Saini,¹⁵ J. Salamanca,¹⁸ C. Salgado,³⁰ A. Sandorfi,⁴¹ J. P. Santoro,^{44,8,41} V. Sapunenko,⁴¹ D. Schott,¹⁴ R. A. Schumacher,⁷ V. S. Serov,²¹ Y. G. Sharabian,⁴¹ D. Sharov,³⁹ N. V. Shvedunov,³⁹ E. S. Smith,⁴¹ L. C. Smith,⁴⁵ D. I. Sober,⁸ D. Sokhan,¹² A. Starostin,⁵ A. Stavinsky,²¹ S. Stepanyan,⁴¹ S. S. Stepanyan,²⁶ B. E. Stokes,^{15,16} P. Stoler,³⁵ K. A. Stopani,³⁹ I. I. Strakovsky,¹⁶ S. Strauch,^{16,40} M. Taiuti,¹ D. J. Tedeschi,⁴⁰ A. Teymurazyan,²⁴ A. Tkabladze,^{33,16} S. Tkachenko,³⁴ L. Todor,³⁷ C. Tur,⁴⁰ M. Ungaro,^{35,11} M. F. Vineyard,⁴² A. V. Vlassov,²¹ D. P. Watts,¹² X. Wei,⁴¹ L. B. Weinstein,³⁴ D. P. Weygand,⁴¹ M. Williams,⁷ E. Wolin,⁴¹ M. H. Wood,⁴⁰ A. Yegneswaran,⁴¹ M. Yurov,²⁶ L. Zana,²⁹ J. Zhang,³⁴ B. Zhao,¹¹ and Z. W. Zhao⁴⁰

(CLAS Collaboration)

¹*Istituto Nazionale di Fisica Nucleare, Sezione di Genova, 16146 Genova, Italy*

²*Physics Department and Nuclear Theory Center, Indiana University, Bloomington, Indiana 47405, USA*

³*Argonne National Laboratory, Argonne, Illinois 60439, USA*

⁴*Arizona State University, Tempe, Arizona 85287-1504, USA*

⁵*University of California at Los Angeles, Los Angeles, California 90095-1547, USA*

⁶*California State University, Dominguez Hills, Carson, California 90747, USA*

⁷*Carnegie Mellon University, Pittsburgh, Pennsylvania 15213, USA*

⁸*Catholic University of America, Washington, D.C. 20064, USA*

⁹*CEA-Saclay, Service de Physique Nucléaire, 91191 Gif-sur-Yvette, France*

¹⁰*Christopher Newport University, Newport News, Virginia 23606, USA*

¹¹*University of Connecticut, Storrs, Connecticut 06269, USA*

¹²*Edinburgh University, Edinburgh EH9 3JZ, United Kingdom*

¹³*Fairfield University, Fairfield Connecticut 06824, USA*

¹⁴*Florida International University, Miami, Florida 33199, USA*

¹⁵*Florida State University, Tallahassee, Florida 32306, USA*

- ¹⁶The George Washington University, Washington, D.C. 20052, USA
¹⁷University of Glasgow, Glasgow G12 8QQ, United Kingdom
¹⁸Idaho State University, Pocatello, Idaho 83209, USA
¹⁹INFN, Laboratori Nazionali di Frascati, 00044 Frascati, Italy
²⁰Institut de Physique Nucleaire ORSAY, Orsay, France
²¹Institute of Theoretical and Experimental Physics, Moscow, 117259, Russia
²²Institute for High Energy Physics, Protvino, 142281, Russia
²³James Madison University, Harrisonburg, Virginia 22807, USA
²⁴University of Kentucky, Lexington, Kentucky 40506, USA
²⁵Kharkov Institute of Physics and Technology, Kharkov 61108, Ukraine
²⁶Kyungpook National University, Daegu 702-701, Republic of Korea
²⁷University of Massachusetts, Amherst, Massachusetts 01003, USA
²⁸Henryk Niewodniczanski Institute of Nuclear Physics PAN, 31-342 Krakow, Poland
²⁹University of New Hampshire, Durham, New Hampshire 03824-3568, USA
³⁰Norfolk State University, Norfolk, Virginia 23504, USA
³¹University of North Carolina, Wilmington, North Carolina 28403, USA
³²North Carolina Agricultural and Technical State University, Greensboro, North Carolina 27455, USA
³³Ohio University, Athens, Ohio 45701, USA
³⁴Old Dominion University, Norfolk, Virginia 23529, USA
³⁵Rensselaer Polytechnic Institute, Troy, New York 12180-3590, USA
³⁶Rice University, Houston, Texas 77005-1892, USA
³⁷University of Richmond, Richmond, Virginia 23173, USA
³⁸The Institute of Physical and Chemical Research, RIKEN, Wako, Saitama 351-0198, Japan
³⁹Skobel'syn Nuclear Physics Institute, Skobel'syn Nuclear Physics Institute, 119899 Moscow, Russia
⁴⁰University of South Carolina, Columbia, South Carolina 29208, USA
⁴¹Thomas Jefferson National Accelerator Facility, Newport News, Virginia 23606, USA
⁴²Union College, Schenectady, New York 12308, USA
⁴³Universidad Técnica Federico Santa María, Valparaíso, Chile
⁴⁴Virginia Polytechnic Institute and State University, Blacksburg, Virginia 24061-0435, USA
⁴⁵University of Virginia, Charlottesville, Virginia 22901, USA
⁴⁶College of William and Mary, Williamsburg, Virginia 23187-8795, USA
⁴⁷Yerevan Physics Institute, 375036 Yerevan, Armenia

(Received 11 November 2008; published 11 March 2009)

We report on the results of the first measurement of exclusive $f_0(980)$ meson photoproduction on protons for $E_\gamma = 3.0\text{--}3.8$ GeV and $-t = 0.4\text{--}1.0$ GeV². Data were collected with the CLAS detector at the Thomas Jefferson National Accelerator Facility. The resonance was detected via its decay in the $\pi^+\pi^-$ channel by performing a partial wave analysis of the reaction $\gamma p \rightarrow p\pi^+\pi^-$. Clear evidence of the $f_0(980)$ meson was found in the interference between P and S waves at $M_{\pi^+\pi^-} \sim 1$ GeV. The S -wave differential cross section integrated in the mass range of the $f_0(980)$ was found to be a factor of about 50 smaller than the cross section for the ρ meson. This is the first time the $f_0(980)$ meson has been measured in a photoproduction experiment.

DOI: 10.1103/PhysRevLett.102.102001

PACS numbers: 13.60.Le, 11.80.Et, 14.40.Cs

The spectroscopy of low-lying scalar mesons is a topic of high interest in hadronic physics. Experimental and theoretical evidence indicates that these states make a full $SU(3)$ flavor nonet. However, the mass spectrum ordering of the σ , κ , $f_0(980)$, and $a_0(980)$ mesons disfavors the naive $q\bar{q}$ picture. The most natural explanation for this multiplet with an inverted mass spectrum is that these mesons are diquark-antidiquark bound states with correct mass ordering [1,2]. Recent advances in the application of chiral effective field theory with dispersion relations [3–6] has led to extensive investigation of the subject.

So far, scalar mesons have been observed in hadron-hadron collisions, $\gamma\gamma$ collisions in decays of various mesons such as ϕ , J/Ψ , D and B while very few studies with

electromagnetic probes were attempted. Their cross sections are relatively small compared to the dominant production of vector mesons; however, S -wave parameters can be extracted by performing a partial wave analysis and exploiting the interference with the dominant P waves. The dependence of the cross section on the momentum transfer t and resonance mass might shed light on the peculiar structure of these mesons. For example, the authors of Ref. [7] suggest that a compact $q\bar{q}$ system is expected to be observed as a peak in the invariant mass distribution of the resonance decay products, while a diffuse state, e.g., a meson molecule, would more likely appear as a dip.

The dominant decay mode for most of the light scalar mesons is the $\pi\pi$ channel. Up to now the most compre-

hensive analyses of $\pi^+\pi^-$ photoproduction at few GeV energies were performed at DESY [8,9], SLAC [10,11] and Jefferson Lab [12]. These measurements showed the dominance of the ρ resonance. In the analysis of the SLAC data, the angular dependence was parametrized in terms of P wave alone, and no attempt was made to extract S -wave or higher partial waves. More recently, the HERMES Collaboration investigated the interference of the P wave in $\pi^+\pi^-$ electroproduction (with $Q^2 > 3 \text{ GeV}^2$) with the S and D waves [13].

In this work we focus on $\pi^+\pi^-$ photoproduction at photon energies between 3.0 and 3.8 GeV in the range of momentum transfer squared $-t$ between 0.4 and 1.0 GeV^2 and present the first analysis of the S -wave photoproduction of pion pairs in the region of the $f_0(980)$.

The present measurement was performed using the CLAS detector (CEBAF Large Acceptance Spectrometer) [14] at Jefferson Lab in experimental Hall B with a bremsstrahlung photon beam produced by a primary electron beam of energy $E_0 = 4.0 \text{ GeV}$ hitting a gold foil of 10^{-4} radiation lengths. A bremsstrahlung tagging system with an energy resolution of 0.1% E_0 was used to tag photons in the energy range 3.0–3.8 GeV. The target consisted of a 40-cm-long cylindrical cell containing liquid hydrogen at 20.4 K. The high-intensity photon flux ($\sim 10^7 \gamma/s$) was measured by dedicated devices with a systematic uncertainty of 10%.

Outgoing hadrons were detected and identified in CLAS. Charged particle trajectories were bent by a toroidal magnetic field ($\sim 0.5 \text{ T}$), which is generated by six superconducting coils. Momentum information was obtained via tracking through three regions of multiwire drift chambers. The CLAS momentum resolution for charged particles is approximately 0.5%–1% (σ) depending on the kinematics. The detector geometrical acceptance for each positive particle in the relevant kinematic region is about 40%. Time-of-flight scintillators were used for hadron identification. The interaction time of the incoming photon in the target was measured by detecting the outgoing particles in the Start Counter [15]. Coincidences between the photon tagger and two charged particles in the CLAS detector triggered the recording of the events.

The exclusive reaction $\gamma p \rightarrow p f_0(980)$ was measured via the most sizable $f_0(980)$ decay mode ($f_0(980) \rightarrow \pi^+\pi^-$ with $\Gamma(\pi\pi)/[\Gamma(\pi\pi) + \Gamma(K\bar{K})] \sim 75\%$ [16]). The final state was selected requiring detection of both the proton and the π^+ in CLAS and reconstructing the π^- using the missing-mass technique [17]. In this analysis the momentum transfer $-t$ was limited to the range 0.4–1.0 GeV^2 where the product of the detector acceptance and the reaction yield is larger. About 40 M events were identified after all selection cuts. Calibrations of all detector components were performed, achieving a precision of a few MeV in the invariant dipion mass determination. An experimental resolution of a similar magnitude was evaluated from Monte Carlo simulation.

The data analysis consisted of two main steps: (i) extraction of moments $\langle Y_{LM} \rangle$ of the dipion angular distributions; (ii) fit of the moments with a parametrization of the partial waves. In the following, we briefly outline the procedure, referring to a more comprehensive paper [18] for analysis details.

Moments $Y_{LM}(\Omega_\pi)$ are defined as the projection of the production cross section on spherical harmonics with defined angular momentum L and z component M :

$$\langle Y_{LM} \rangle(E_\gamma, t, M_{\pi\pi}) = \sqrt{4\pi} \int d\Omega_\pi Y_{LM}(\Omega_\pi) \times \frac{d\sigma}{dt dM_{\pi\pi} d\Omega_\pi}, \quad (1)$$

where E_γ is the photon energy, t the invariant momentum transfer to the dipion system squared, and $M_{\pi\pi}$ its mass. The decay angles $\Omega_\pi = (\theta_\pi, \phi_\pi)$ are the polar and azimuthal angles of the π^+ in the helicity rest frame.

The extraction of the moments from data requires that the measured angular distributions are corrected by acceptance. The CLAS acceptance and reconstruction efficiency were evaluated with Monte Carlo simulations. Events were generated according to three-particle phase space in the same photon energy range as the experiment, processed by a GEANT-based code that included knowledge of the detector geometry and response to traversing particles, and reconstructed using the same analysis procedure that was applied to the data. Moments were expanded in a model-independent way in two sets of basis functions and, after weighting with Monte Carlo simulations, they were fitted to the data by maximizing a likelihood function built on an event-by-event basis. In the first case, the parametrization was given in terms of *amplitudes*, while in the second, *moments* were directly used [19]. In both cases the number of basis functions was limited for practical reasons. In the kinematic range $3.0 < E_\gamma < 3.8 \text{ GeV}$, $0.4 < -t < 1.0 \text{ GeV}^2$ and $0.4 < M_{\pi\pi} < 1.4 \text{ GeV}$, moments with $L \leq 4$ and $|M| \leq L$ were calculated as an average of results obtained with the two parametrizations.

Detailed systematic studies were performed using both Monte Carlo simulations and real data to ensure the validity of the approximations and to study possible effects related to the basis truncation and the detector acceptance. The comparison of results obtained by the different methods was used to estimate the systematic uncertainty related to the analysis procedure. We found that the variation in the moments obtained from the different procedures is larger than the statistical uncertainty and larger than other sources of systematic uncertainty, such as event selection cuts, detector resolution and inefficiency. The final uncertainty was then obtained by summing in quadrature the fit uncertainty given by MINUIT, the uncertainty associated with the photon flux determination, and the above-mentioned uncertainty on the moment extraction procedure.

The plots in Fig. 1 show the moments $\langle Y_{00} \rangle$, $\langle Y_{10} \rangle$ and $\langle Y_{11} \rangle$ in a selected E_γ and t bin. Moment $\langle Y_{00} \rangle$ corresponds to the differential cross section $d\sigma/dtdM_{\pi\pi}$. As expected this is dominated by the contribution of the ρ meson in the P wave shown by the prominent peak at $M_{\pi\pi} \sim 0.77$ GeV. In moments $\langle Y_{10} \rangle$ and $\langle Y_{11} \rangle$, the contribution of the S wave is maximum and enters via interference with the dominant P wave.

The second step of the analysis consisted of extracting the partial wave amplitudes from the angular moments. These can be expressed as bilinear in terms of the amplitudes $a_{lm} = a_{lm}(\lambda, \lambda', \lambda_\gamma, E_\gamma, t, M_{\pi\pi})$ with angular momentum l and z projection m (in the chosen reference system m coincides with the helicity of the dipion system):

$$\langle Y_{LM} \rangle \propto \sum_{l'm', lm, \lambda, \lambda'} C(l'm', lm, LM) a_{lm} a_{l'm'}^* \quad (2)$$

where λ and λ' are the initial and final nucleon helicity, respectively, λ_γ is the helicity of the photon, and C are Clebsch-Gordan coefficients. Each amplitude was expressed as a linear combination of $\pi\pi$ amplitudes of fixed isospin, $a_{lm,I}$ with $I = 0, 1, 2$. The number of waves was reduced restricting the analysis to $|m| \leq 1$, since $m = 2$ waves are expected to be small in the mass range under investigation.

Using a dispersion relation [20], the helicity amplitude $a_{lm,I}$ was expressed in terms of the scattering matrix elements of $\pi\pi$ scattering, chosen to reproduce the known phase shifts, inelasticities [6,16], and the isoscalar ($l = S, D$), isovector ($l = P, F$) and isotensor ($l = S, D$) amplitudes in the range $0.4 \text{ GeV} < \sqrt{s} < 1.4 \text{ GeV}$. With this approach, our ignorance about the production process is gathered in a reduced amplitude, $\tilde{a}_{lm,I}$, which does not have singularities for $s > 4m_\pi^2$ and can be expanded in a polynomial function. This was chosen to be of second order and its coefficients are the partial wave analysis parameters that were extracted by the simultaneous fit of the angular moments defined in Eq. (2). All amplitudes but the scalar-isoscalar are saturated by the $\pi\pi$ state. For the scalar-isoscalar amplitude, the $K\bar{K}$ channel was also included. A detailed discussion of the approximations used in the analysis and of the dispersion relation equation are reported in Ref. [18].

Partial waves a_{lm} up to $l = 3$ (F wave) were determined fitting all moments $\langle Y_{LM} \rangle$ with $L \leq 4$ and $|M| \leq \min(L, 2)$. Results of the fit are shown as a gray band in Fig. 1 on top of the experimental angular moments $\langle Y_{00} \rangle$, $\langle Y_{10} \rangle$ and $\langle Y_{11} \rangle$ in a selected E_γ and t bin. As stated above, the contribution of the S wave is maximum in moments $\langle Y_{10} \rangle$ and $\langle Y_{11} \rangle$. In particular the large structure at the ρ mass in $\langle Y_{11} \rangle$ is due to the interference of the S wave with the dominant, helicity-non-flip wave, $P_{m=1}$ ($\lambda_\gamma = 1 \rightarrow m = 1$). In moment $\langle Y_{10} \rangle$ the same structure is due to the interference with the $P_{m=0}$ wave, corresponding to one unit of helicity flip ($\lambda_\gamma = 1 \rightarrow m = 0$). A second dip near

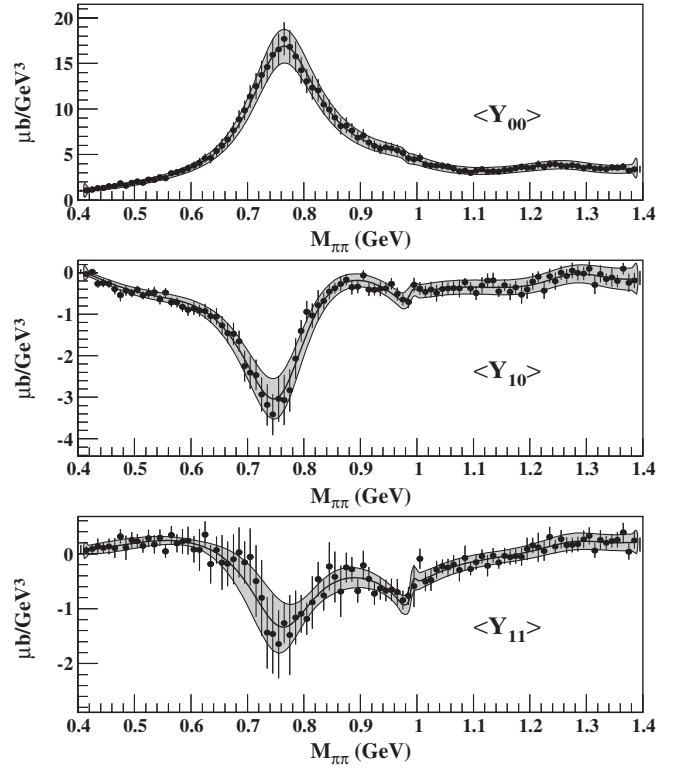


FIG. 1. Selected angular moments in the photon energy bin $3.2 < E_\gamma < 3.4 \text{ GeV}$ and momentum transfer $0.5 < -t < 0.6 \text{ GeV}^2$. Error bars include the systematic uncertainty related to the photon flux normalization and the moment extraction procedure. The gray band shows the result of the fit of the moments in terms of partial wave amplitudes.

$M_{\pi\pi} = 1 \text{ GeV}$ is clearly visible and corresponds to the direct production of a resonance that we interpret as the $f_0(980)$. The mass and width of this structure are compatible with the PDG values ($M = 980 \pm 10 \text{ MeV}$ and $\Gamma = 40\text{--}100 \text{ MeV}$ [16]).

It should be noted that moments of the $\pi^+\pi^-$ angular distribution can be affected by baryon resonances decaying to π^+p and π^-p . These contributions represent a background for our analysis but, having a smooth dependence on the di-pion mass, they cannot create narrow structures in these observables. In addition, they are expected to be small for low moments and limited values of $M_{\pi\pi}$ ($\lesssim 1.1 \text{ GeV}$) that are the focus of this analysis.

The P and S partial wave differential cross sections $d\sigma/dtdM_{\pi\pi}$ are shown in Fig. 2. As expected, the S -wave photoproduction is suppressed compared to the P wave, which is dominated by the ρ meson.

The S wave shows a clear variation in the vicinity of the $f_0(980)$. However, the resonance component seems to be embedded in a coherent background. The evidence of the $f_0(980)$ signal in the S wave is a sign that photoproduction may indeed be a good tool for accessing meson resonances other than vector meson states. The total S -wave differential cross section $d\sigma/dt$ in the region of the $f_0(980)$ was

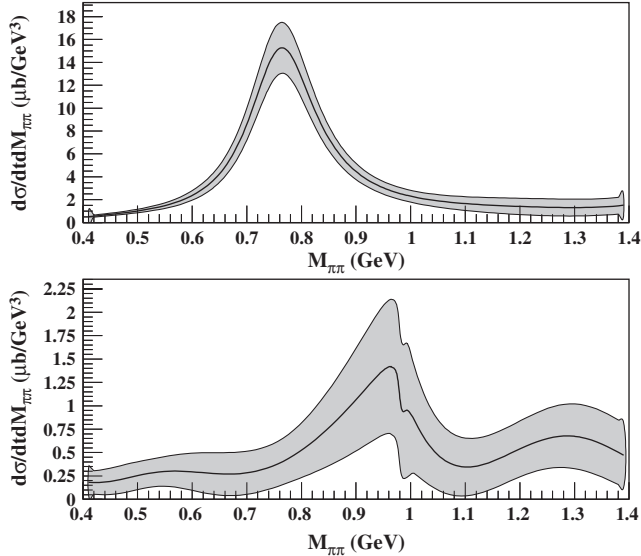


FIG. 2. Partial wave cross sections in the same kinematic bin as Fig. 1. The top and bottom panels show the P and the S wave, respectively. The width of the bands represents the uncertainty estimated as explained in the text.

obtained integrating the $M_{\pi\pi}$ mass in the range 0.98 ± 0.04 GeV. Differential cross sections $d\sigma/dt$ in $E_\gamma = 3.4 \pm 0.4$ GeV for S wave (open circles), obtained as described above, and P wave (solid dots), integrated in the ρ mass range ($M_{\pi\pi} = 0.4$ – 1.2 GeV), are shown in Fig. 3. The S -wave cross section is found to be a factor of about 50 smaller than the cross section for the P wave.

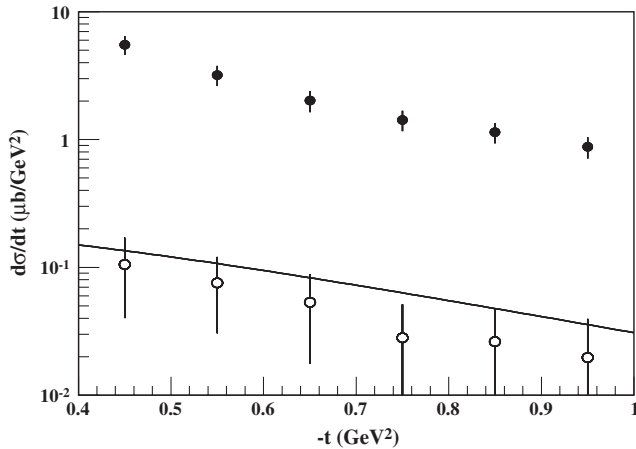


FIG. 3. Partial wave differential cross sections $d\sigma/dt$ in the photon energy range $E_\gamma = 3.0$ – 3.8 GeV, for the P wave (solid dots) and S wave (open circles) integrated in the $M_{\pi\pi}$ mass range 0.4 – 1.2 GeV and 0.98 ± 0.04 GeV, respectively. The error bars include statistical and systematic uncertainties summed in quadrature. The line is a model prediction for the S wave from Refs. [21,22]. Data suggest a change in slope around $-t = 0.8$ GeV², indicative of a possible interference between different production mechanisms. In the case of ρ photoproduction this effect was also seen at higher energies [25].

The solid line is a prediction for the S wave of a model based on Regge exchanges [21,22]. This was normalized to DESY K^+K^- photoproduction data [23] and was able to reproduce the S -wave measured in the same channel at Daresbury [24]. The agreement of the calculation with our data suggests that the $\pi^+\pi^-$ S -wave cross section extracted here is consistent with the measurement in the K^+K^- channel. It also indicates that the present data can be used in phenomenological analyses that, exploiting the pointlike nature of photon interactions, will provide information about the resonance structure and production mechanisms.

In summary, we measured $\pi^+\pi^-$ photoproduction in the photon energy range $E_\gamma = 3.0$ – 3.8 GeV and momentum transfer range 0.4 GeV² $< -t < 1.0$ GeV² performing a partial wave analysis. Moments of the dipion angular distribution were parametrized in terms of production amplitudes, expressed as bilinear in the partial waves, and fitted to the experimental data. The systematic uncertainty related to the whole procedure was estimated performing the analysis using different procedures and approximations. As expected, the dominant partial wave was found to be the one associated with the helicity-non-flip $\rho(770)$ production. The interference between P and S waves at $M_{\pi\pi} \sim 1$ GeV clearly indicates the presence of the $f_0(980)$ resonance. This is the first time the $f_0(980)$ meson has been measured in a photoproduction experiment.

We would like to acknowledge the outstanding efforts of the staff of the Accelerator and the Physics Divisions at Jefferson Lab that made this experiment possible. This work was supported in part by the Italian Istituto Nazionale di Fisica Nucleare, the French Centre National de la Recherche Scientifique and Commissariat à l'Énergie Atomique, the U.S. Department of Energy and National Science Foundation, and the Korea Science and Engineering Foundation. Jefferson Science Associates, LLC, operates Jefferson Lab for the United States Department of Energy under U.S. DOE contract DE-AC05-06OR23177.

-
- [1] R.L. Jaffe, Phys. Rev. D **15**, 281 (1977).
 - [2] L. Maiani, F. Piccinini, A. D. Polosa, and V. Riquer, Phys. Rev. Lett. **93**, 212002 (2004).
 - [3] G. Colangelo, J. Gasser, and H. Leutwyler, Nucl. Phys. **B603**, 125 (2001).
 - [4] J.R. Pelaez and F.J. Yndurain, Phys. Rev. D **71**, 074016 (2005); J.R. Pelaez, Phys. Rev. Lett. **92**, 102001 (2004).
 - [5] M.R. Pennington, Phys. Rev. Lett. **97**, 011601 (2006).
 - [6] J.A. Oller, E. Oset, and J.R. Pelaez, Phys. Rev. D **59**, 074001 (1999).
 - [7] I.J.R. Aitchison and M.G. Bowler, J. Phys. G **3**, 1503 (1977).
 - [8] R. Erbe *et al.*, Phys. Rev. **175**, 1669 (1968).
 - [9] W. Struczinski *et al.*, Nucl. Phys. **B108**, 45 (1976).
 - [10] J. Ballam *et al.*, Phys. Rev. D **5**, 545 (1972).

- [11] J. Ballam *et al.*, Phys. Rev. D **7**, 3150 (1973).
- [12] M. Battaglieri *et al.*, Phys. Rev. Lett. **87**, 172002 (2001).
- [13] A. Airapetian *et al.*, Phys. Lett. B **599**, 212 (2004).
- [14] B. Mecking *et al.*, Nucl. Instrum. Methods Phys. Res., Sect. A **503**, 513 (2003) and references therein.
- [15] Y. G. Sharabian *et al.*, Nucl. Instrum. Methods Phys. Res., Sect. A **556**, 246 (2006).
- [16] W.-M. Yao *et al.*, J. Phys. G **33**, 1 (2006).
- [17] M. Battaglieri, CLAS-Analysis 2001-002, May 2001, <http://www.jlab.org/Hall-B/pubs/analysis/01-002.ps>.
- [18] M. Battaglieri *et al.*, Phys. Rev. D (to be published).
- [19] G. Grayer *et al.*, Nucl. Phys. **B75**, 189 (1974).
- [20] J. L. Basdevant and E. L. Berger, Phys. Rev. Lett. **37**, 977 (1976).
- [21] L. Bibrzycki, L. Lesniak, and A. P. Szczepaniak, Eur. Phys. J. C **34**, 335 (2004).
- [22] C. R. Ji, R. Kaminski, L. Lesniak, A. Szczepaniak, and R. Williams, Phys. Rev. C **58**, 1205 (1998).
- [23] H.-J. Behrend *et al.*, Nucl. Phys. **B144**, 22 (1978).
- [24] D. P. Barber *et al.*, Z. Phys. C **12**, 1 (1982).
- [25] J. Breitweg *et al.*, Eur. Phys. J. C **14**, 213 (2000).